

# Disk Diffusion Propagation Model for the Outburst of XTE J1118+480

Kent S. Wood<sup>1</sup>, Lev Titarchuk<sup>1,2</sup>, Paul S. Ray<sup>1</sup>, Michael T. Wolff<sup>1</sup>, Michael N. Lovellette<sup>1</sup>  
 & Reba M. Bandyopadhyay<sup>3</sup>

## ABSTRACT

We present a linear diffusion model for the evolution of the double-peaked outburst in the transient source XTE J1118+480. The model treats the two outbursts as episodic mass deposition at the outer radius of the disk followed by evolution of disk structure according to a diffusion process. We demonstrate that light curves with fast-rise, exponential decay profile are a general consequence of the diffusion process. Deconvolution of the light curve proves to be feasible and gives an input function specifying mass deposition at the outer disk edge as well as the total mass of the disk, both as functions of time. The derived evolution of total disk mass can be correlated with the observed evolution of the  $\sim 0.1$  Hz QPO in the source reported in Wood et al. (2000).

*Subject headings:* accretion — black hole physics — binaries: close — stars: individual (XTE J1118+480)

## 1. Introduction

X-ray novae (XN), also called Soft X-ray Transients (SXTs), are binary X-ray sources that show outburst behavior (Chen et al. 1997). The prevailing theory for their transient behavior is based on the disk instability model (DIM) first proposed to explain dwarf novae outbursts (see the extensive review by Lasota 2001). Applying this model to XN requires significant modifications due to X-ray irradiation from the central disk and the disruption of the inner disk, presumably by an advection dominated accretion flow (ADAF), in quiescence. The DIM with these modifications is shown to be quite successful in modeling transient outbursts similar to the canonical XN A0620–00 (Dubus et al. 2001). However, it is also

---

<sup>1</sup>E. O. Hulbert Center for Space Research, Naval Research Laboratory, Washington, DC 20375

<sup>2</sup>George Mason University/CEOSR, Fairfax, VA 22030

<sup>3</sup>NRL/NRC Research Associate

clear that some sources undergo outbursts that are very difficult to reconcile with the DIM. In this paper we consider one such source, XTE J1118+480, and develop an alternative model for the outburst based on modulated mass transfer into the outer disk, rather than a sudden increase in viscosity in a pre-existing disk as in the DIM.

We derive a general prescription for calculating X-ray outburst light curves based on a diffusion propagation model in the disk. We begin with the same basic diffusion equations as Bath & Pringle (1981, hereafter BP81) but we derive an analytical solution rather than solving the equations numerically. We derive a Green's function from the first outburst and develop a deconvolution technique to calculate the mass input rate as a function of time for the second outburst. This allows us to derive the time evolution of the mass of the disk for the second outburst. Based on the global oscillation model of Titarchuk & Osherovich (2000, hereafter TO00) we expect the QPO to correlate inversely with the disk mass. This provides us with at least one observational test for the model.

It is possible that this model may be applicable to outbursts observed in other sources as well. Brocksopp et al. (2000) point out similarities among five XNe: GRO J0422+32, XTE J1118+480, X1354-644, GRO J1719-24, and GS 2023+338. All five have had at least one outburst in which the source remains in the low-hard state through the entire episode. In three instances a  $\sim 0.1 - 0.5$  Hz QPO drifting persistently upward in frequency is seen. These sources may be good candidates for future tests of this model; however, in this paper we limit ourselves to XTE J1118+480 as an example.

In Section 2 we review the properties of the source, particularly the features of the 2000 outburst which are difficult to account for in the DIM. In Section 3 we describe the main features of the diffusion model. In Section 4 we solve for the Green's function for the specific case where  $\psi = 2$  and in the general case. In Section 5 we derive the deconvolution procedure to get the accretion rate into the disk and the time evolution of the disk mass during the outburst. We apply the full procedure to the data on XTE J1118+480 in Section 6. In Section 7 we show that this model can explain the time evolution of the low-frequency quasi-periodic oscillation (QPO) seen during most of the outburst. We conclude in Section 8 with a discussion of the successes and limitations of this model.

## 2. The X-ray Nova XTE J1118+480

XTE J1118+480 is a black hole (BH) transient that was observed from radio to hard X-rays during 2000 January to August. Optical observations after the source returned to quiescence confirmed the black hole nature of the compact object by measuring a mass func-

tion of  $f(M) = 6.0 \pm 0.36 M_{\odot}$  (McClintock et al. 2000; Wagner et al. 2001). This is among the highest mass functions measured for any transient. In addition, the combination of the small distance to the source ( $1.8 \pm 0.6$  kpc; McClintock et al. 2000) and the high Galactic latitude ( $b = 62^{\circ}$ ) results in this source having the lowest reddening of any XN. The X-ray light curve of the source is peculiar, with an unusual *double* outburst (see Figure 1). The first outburst appears to have a fast rise followed by an exponential decay (FRED morphology), but the second outburst is irregular with multiple maxima. The X-ray spectrum was essentially constant as an absorbed power law with photon spectral index of 1.73 (Wood et al. 2000), typical of the low/hard state of black holes. A radio counterpart at 5 GHz has been detected during outburst, although jets were not directly resolved with MERLIN to a limit of  $< 65$  ( $d/\text{kpc}$ ) AU (Fender et al. 2000).

An earlier paper (Wood et al. 2000) reported detailed evolution of the 0.1 Hz QPO, using X-ray data from the USA Experiment and *RXTE*. The QPO frequency increased monotonically from 0.07 to 0.15 Hz over  $\sim 2$  months, failing to correlate with the X-ray luminosity which rises and falls over the same interval. In this paper, we explore using the disk mass rather than usual quantities (such as luminosity or spectral parameters) to correlate with the drifting QPO frequency. The low ( $\sim 0.1$  Hz) frequency suggests an origin at a large radius in the disk because dynamical timescales scale roughly with the Kepler frequency. One theory that could explain such a low-frequency QPO is the global oscillation model of TO00. Their model describes a large-scale coherent oscillation in the outer disk, linking QPO issues to those of overall disk structure. The model leads to a BH mass estimate for XTE J1118+480 of  $\sim 7 M_{\odot}$  based on the  $\sim 0.1$  Hz QPO frequency, in agreement with recent optical data (Wagner et al. 2001) which suggest a BH mass range of  $6.0\text{--}7.7 M_{\odot}$ . (We note that there is a typographical error in equation (14) of TO00 which should have  $x_{\text{in}}^{-4/5}$  instead of  $x_{\text{in}}^{-8/15}$ .) The same QPO was seen in EUV and optical wavelengths (Haswell et al. 2000; Hynes et al. 2000).

The double outburst profile of this source is difficult to account for in the standard DIM. If an outburst is triggered by a sudden increase in disk viscosity and leads to the FRED-type outburst in 2000 January, how can another outburst, with five times the fluence, occur so shortly afterwards? What mechanism turns off the first outburst? And, why does the second outburst have such an irregular shape? If the instability is triggered at some maximum value of the disk mass, and the amount of mass consumed in the first outburst was replenished in  $\sim 30$  days, then the mass consumed in the second outburst should be replenished at about 0.5 years. Thus, the DIM models would have predicted that another outburst should have occurred by now. Our alternative model is that the outbursts were fueled by sporadic mass transfer from the companion rather than from a large amount of mass stored in the disk during quiescence. It is beyond the scope of the current paper to develop the dynamics of

the mass transfer which accounts for this behavior. It is instructive to look at the energetics of the outburst. The luminosity of the long outburst was about  $3 \times 10^{35}$  erg/s (for a distance of 1.8 kpc) which is only  $1.4 \times 10^{-4} L_{\text{Edd}}$  (for an assumed black hole mass of  $7M_{\odot}$ ), whereas the canonical DIM outbursts approach the Eddington limit at their peak.

Mass transfer modulation models for XN outbursts have previously been considered as viable alternatives to the DIM. As the XTE J1118+480 outbursts are not easily reconciled with the standard DIM, it seems reasonable to develop a different model for this source. For example, Kuulkers (2001) has suggested that the long outburst of XTE J1118+480 is a superoutburst of the type seen in the SU UMa class of cataclysmic variables (Warner 1995), based on striking similarities in the X-ray and optical lightcurves and the appearance of superhumps. To account for some of the unusual aspects of XTE J1118+480, here we investigate an alternative model where the outburst is driven by mass transfer from the companion and the diffusive propagation of material in the disk.

### 3. Description of the Diffusion Model: Equations and Boundary Conditions

We now derive the main equation describing diffusive propagation of matter in the disk. Using the angular momentum balance [e.g. Shakura & Sunyaev 1973, see also Titarchuk & Osherovich 1999 hereafter (TO99), eq. 4]

$$\dot{M} = 2\pi \frac{d(W_{r\varphi} R^2)}{d(\omega R^2)} \quad (1)$$

and the continuity equation

$$\frac{\partial \Sigma}{\partial t} = \frac{1}{2\pi R} \frac{\partial \dot{M}}{\partial R} + Q(R, t) \quad (2)$$

where  $\dot{M}(R, t)$  and  $Q(R, t)$  are the mass accretion in the disk and mass accretion input over the disk at the given radius  $R$  and at the given time  $t$ , and  $W_{r\varphi}$  is the  $r\varphi$ -component of a viscous stress tensor  $W$ . We can get a relation between  $W_{r\varphi}$  and the surface density  $\Sigma(r, t)$  using equation (5) in TO99 with an assumption that the rotational frequency is equal to the Keplerian one,  $\omega = \omega_{\text{K}}$ :

$$W_{r\varphi} = -2\eta H R \frac{\partial \omega_{\text{K}}}{\partial R} = (3/2)(GM_x)^{1/2} \nu \Sigma R^{-3/2} \quad (3)$$

where  $H$  is a half-thickness of a disk,  $G$  is the gravitational constant,  $M_x$  is the mass of the central object,  $\eta = \rho\nu$  is a viscosity,  $\rho$  is the density,  $\nu = l_t v_t / 3$  is a kinematic viscosity in the disk and  $l_t$ ,  $v_t$  are the turbulent scale and velocity in the disk respectively. We also use the relation  $\Sigma = 2H\rho$ .

A relation between  $\dot{M}$  and  $\Sigma$  can be obtained using equation (1) and (3) with an assumption that  $\omega = \omega_K$

$$\dot{M} = 2\pi \times 3R^{1/2} \frac{\partial}{\partial R} [\nu \Sigma R^{1/2}]. \quad (4)$$

Substitution of  $\dot{M}$  from this equation into equation (2) leads to the diffusion equation

$$\frac{\partial \Sigma}{\partial t} = \mathbf{\Lambda}_R \Sigma = \frac{3}{R} \frac{\partial}{\partial R} \left( R^{1/2} \frac{\partial}{\partial R} [\nu \Sigma R^{1/2}] \right) + Q(R, t). \quad (5)$$

Equation (5) is identical to equation (2.3) of BP81. It is worth noting that the derivation presented here and BP81 is general, using only the mass and angular momentum conservations and an assumption of Kepler rotational velocity in the disk. It does not invoke specific assumptions regarding the structure of the disk. The viscosity value,  $\eta = \rho\nu$  implemented for calculation of  $W_{r\varphi}$  in equation (3) are averaged over the vertical size of the disk. The product of  $2H\rho$  is in fact an integral of the density,  $\rho$ , over the  $z$ -coordinate, yielding a surface density  $\Sigma$ .

In our calculation we will assume that the mass accretion input (presumably from the companion) occurs at the outer boundary of the disk at  $R = R_0$ , namely

$$Q(R, t) = \frac{A(t)\delta(R - R_0)}{2\pi R}. \quad (6)$$

Thus,  $A(t)$  is the mass input rate as a function of time at the outer edge of the disk. Using equations (2) and (6) we derive the differential equation for the disk mass  $M_d = 2\pi \int_{R_{in}}^{R_0} \Sigma R dR$ :

$$\frac{\partial M_d}{\partial t} = \dot{M}(R_0, t) - \dot{M}(R_{in}, t) + A(t), \quad (7)$$

where mass accretion  $\dot{M}(R_{in}, t)$  at the inner disk boundary can be calculated using equation (4). We assume the reflection boundary at the outer edge of the disk; in other words, the net mass flux  $\dot{M}(R_0, t)$  through the outer boundary is zero:

$$\dot{M}(R_0, t) = 0. \quad (8)$$

This is compatible with the mass input at the outer edge of the disk from eqn. (6) because the mass input is considered to be added just inside the outer radius  $R_0$  where the reflection boundary condition is imposed. Integration of this equation allows us to get  $M_d$  as a function of time  $t$ :

$$M_d(t) = \int_0^t [A(\tau) - \dot{M}(R_{in}, \tau)] d\tau. \quad (9)$$

We replace the function  $\Sigma$  by the function  $y(R, t) = R^{1/2}\nu\Sigma$ . Using eq. (4) the mass accretion  $\dot{M}$  is then expressed through  $y$  as follows

$$\dot{M} = 2\pi \times 3R^{1/2} \frac{\partial y}{\partial R} \quad (10)$$

and the diffusion equation (5) can be written in the form

$$\frac{\partial y}{\partial t} = \frac{3\nu(R)R^{1/2}}{R} \frac{\partial}{\partial R} R^{1/2} \frac{\partial y}{\partial R} + \frac{\nu(R)A(t)\delta(R - R_0)}{2\pi R^{1/2}}. \quad (11)$$

We combine this equation with the boundary condition at the outer boundary

$$\frac{\partial y}{\partial R} = 0 \quad \text{at} \quad R = R_0 \quad (12)$$

which follows from equations (8, 10). We assume that at the inner boundary  $R_{\text{in}} \ll R_0$ ,  $\Sigma = 0$ , which is equivalent to

$$y = 0 \quad \text{at} \quad R = R_{\text{in}}. \quad (13)$$

Introduction of a new variable  $x = R^{1/2}$  reduces the main equation (11) to:

$$\frac{\partial y}{\partial t} = \mathbf{\Lambda}_x y = \frac{3\nu(x)}{4x^2} \frac{\partial^2 y}{\partial x^2} + \frac{\nu(x)A(t)\delta(x - x_0)}{\pi} \quad (14)$$

with the boundary conditions

$$\frac{\partial y}{\partial x} = 0 \quad \text{at} \quad x = x_0, \quad (15)$$

and

$$y = 0 \quad \text{for} \quad x \rightarrow 0. \quad (16)$$

One can check by direct substitution that the solution of this boundary problem for the inhomogeneous equation (14) can be presented through the following convolution

$$y(x, t) = \int_0^t A(\tau) V(x, t - \tau) d\tau \quad (17)$$

where  $V$  satisfies the homogeneous equation

$$\frac{\partial V}{\partial t} = \mathbf{\Lambda}_x V = \frac{3\nu(x)}{4x^2} \frac{\partial^2 V}{\partial x^2} \quad (18)$$

with the initial condition

$$V(x) = \frac{\nu(x)\delta(x - x_0)}{\pi} \quad \text{at} \quad t = \tau \quad (19)$$

and boundary conditions (15-16). Because our ultimate goal is to find the X-ray luminosity, which is presumably related to the energy release of the accreting matter at the inner disk edge, we will calculate  $\dot{M}$  at  $R = R_{\text{in}}$  (or at  $x \rightarrow 0$ ). We assume that the mass accretion rate at the inner edge is converted with efficiency  $\varepsilon_{\text{eff}}$  into the X-ray luminosity, i.e.  $L_x(t) = \varepsilon_{\text{eff}} \dot{M}(0, t)$ . Thus

$$L_x(t) = \varepsilon_{\text{eff}} \dot{M}(0, t) \propto \dot{M}(0, t) = 3\pi \frac{\partial y}{\partial x} = 3\pi \int_0^t A(\tau) \frac{\partial V(0, t - \tau)}{\partial x} d\tau. \quad (20)$$

#### 4. The analytical solution of the main problem: General and particular cases

The solution  $V(x, t)$  of equation (18) with the initial condition (19) at  $t = 0$  and boundary conditions (15-16) can be presented using separation of variables as a series

$$V(x, t) = \sum_{n=1}^{\infty} e^{-\lambda_n^2 t} \frac{X_n(x) X_n(x_0) p(x_0)}{\|X_n(x)\|^2} \frac{\nu(x_0)}{\pi}, \quad (21)$$

where  $X_n(x)$  and  $\lambda_n$  are eigenfunctions and eigenvalues which can be found from the inhomogeneous ordinary differential equation:

$$X_n'' + \lambda_n^2 p(x) X_n = 0 \quad (22)$$

combined with the boundary conditions

$$X_n = 0 \quad \text{for} \quad x \rightarrow 0, \quad (23)$$

$$\frac{dX_n}{dx} = 0 \quad \text{at} \quad x = x_0. \quad (24)$$

$\|X_n\|$  is the norm of the eigenfunction, which is calculated through the integral (for example, see the derivation of this formula in Titarchuk, Mastichiadis, & Kylafis 1997)

$$\|X_n\|^2 = \int_0^{x_0} p(x) X_n^2(x) dx, \quad (25)$$

where  $p(x) = 4x^2/3\nu(x)$  is the weight function.

Here, we consider a general class of problems where  $\nu(x) = \nu_0 x^\psi$ . In the following sections, we solve the problem for one specific value of  $\psi$ , then present the general solution.

#### 4.1. Case with $\psi = 2$

When the turbulent scale  $l_t$  is proportional to the characteristic scale  $R$  and the turbulent velocity  $v_t$  is independent of radius,  $\psi = 2$  (i.e.  $\nu = \nu_0 R$ ). In this case,

$$X_n(x) = \sin \left[ \frac{2}{(3\nu_0)^{1/2}} \lambda_n x \right], \quad (26)$$

and the eigenvalues  $\lambda_n$  are found from the equation

$$\cos \left[ \frac{2}{(3\nu_0)^{1/2}} \lambda_n x_0 \right] = 0 \quad (27)$$

where the solutions of this equation are

$$\lambda_n = \frac{(3\nu_0)^{1/2}}{2} \frac{\pi(2n-1)}{2x_0}. \quad (28)$$

For this particular case the solution is expressed by harmonics (eqs. [21] and [26])

$$V(x, t) = \frac{2x_0\nu_0}{\pi} \sum_{n=1}^{\infty} \exp[-\pi^2(2n-1)^2t/4t_0] \sin[\pi(2n-1)x/2x_0] \sin[(2n-1)\pi/2] \quad (29)$$

where  $t_0 = 4x_0^2/3\nu_0 = 4R_0^2/3\nu(R_0)$ .  $t_0$  is the viscous timescale and determines both the rise and fall time of the response function.

We define the Green's function  $K(t)$  as the flux through the inner edge of the disk at time  $t$  from delta-function injection at the outer edge at time  $t = 0$ . Thus, it is proportional to  $\partial V(0, t)/\partial x$ :

$$K(t) \propto \frac{\partial V(0, t)}{\partial x} = \nu_0 \sum_{n=1}^{\infty} \exp[-\pi^2(2n-1)^2t/4t_0] (2n-1) \sin[\pi(2n-1)/2]. \quad (30)$$

By definition,  $K(t)$  should be normalized to unity, which can be done analytically in the case  $\psi = 2$ . The integral of the series over  $t$  in this equation is  $\sum_{n=1}^{\infty} (-1)^{n-1} (2n-1)^{-1} = t_0/\pi$ .

The asymptotic form of the series (29) for  $t \ll 4t_0/\pi^2$  can be presented as the integral

$$V(x, t) \simeq \frac{2x_0^2\nu_0}{\pi^2} \int_0^{\infty} \exp[-\lambda^2 x_0^2 t/t_0] \sin(\lambda x) \sin(\lambda x_0) d\lambda, \quad (31)$$

where  $\lambda = \pi(2n-1)/2x_0$  and consequently  $d\lambda = \pi/x_0$ . Transformation of the product of  $\sin(\lambda x) \sin(\lambda x_0)$  into the difference  $[\cos \lambda(x - x_0) - \cos \lambda(x + x_0)]/2$  followed by integration over  $\lambda$  leads us to the formula

$$V(x, t) \simeq \frac{x_0^2\nu_0}{\pi^2} \frac{\pi^{1/2}}{2x_0(t/t_0)^{1/2}} \left\{ \exp[-(x - x_0)^2/4x_0^2(t/t_0)] - \exp[-(x + x_0)^2/4x_0^2(t/t_0)] \right\}. \quad (32)$$

After differentiation we have

$$K(t) \propto \frac{\partial V(0, t)}{\partial x} = \nu_0 \times \frac{1}{2[\pi(t/t_0)]^{3/2}} \exp(-t_0/4t) \quad \text{for } t \ll 4t_0/\pi^2. \quad (33)$$

At large times, we can use the series (30) to get

$$K(t) \propto \frac{\partial V(0, t)}{\partial x} = \nu_0 \times \exp[-\pi^2 t/4t_0] \quad \text{for } t \gg 4t_0/\pi^2. \quad (34)$$

From a combination of the two asymptotic forms (eq. [31,34]) we construct the simple analytical approximation of the Green's function. This combination is a product of the combined exponentials with a linear superposition of the factors before the exponents with weights 1 and 2 respectively:

$$K(t) \simeq C^{-1} [1 + (t_0/\pi t)^{3/2}] \exp[-(t_0/4t + \pi^2 t/4t_0)], \quad (35)$$

where  $C$  is a normalization constant to make the integral of  $K(t)$  equal to unity. We have chosen the weights of the two terms in this approximation to make it more accurately reproduce the series result.

## 4.2. General Case

In this section we investigate the asymptotic behavior of the Green's function for  $t \ll t_0$  and  $t \gg t_0$  in the case of arbitrary kinematic viscosity as a function of  $R$  (or  $x = \sqrt{R}$ ). We have already demonstrated for the  $\psi = 2$  case that the asymptotic for  $t \ll t_0$  is determined by the contribution of terms of the series with  $n \gg 1$  (see eq. [30]). The calculation of the series is reduced to an integral over  $\lambda$  (eq. [31]) where the contribution of terms with  $n$  of order few is negligible. On the other hand, for  $t \gg t_0$  the term with  $n = 1$  is dominant and the contribution of terms with  $n > 1$  is negligible. It is worth noting that the integrated function in equation (31) is a product of an exponent and harmonics. The similar asymptotic form can be obtained in a general case of the kinematic viscosity.

One can check by direct substitution that the eigenfunctions  $X_n(x)$  defined as nontrivial solutions of equations (22–24) have the harmonic asymptotic form for large  $n$

$$X_n(x) = p^{-1/4}(x) \cos[\lambda_n \mu(x) + \varphi] \quad (36)$$

with  $\mu'(x) = d\mu/dx = \sqrt{p(x)}$  when

$$\lambda_n \gg \max_x \left\{ |(p^{1/2})'/p^{1/2}|, |p'/p|, [| (p^{-1/4})''/p |]^{1/2} \right\}. \quad (37)$$

They form an orthogonal set of functions with the squared norm

$$\|X_n\|^2 = \int_0^{x_0} p(x) X_n^2(x) dx = \int_0^{x_0} \mu'(x) \cos^2[\mu(x) + \varphi] dx \simeq \mu(x_0)/2. \quad (38)$$

With an assumption that the kinematic viscosity  $\nu$  is a power law function of the radial coordinate  $x$ , namely  $\nu = \nu_0 x^\psi$ , one can find that  $X_n$  is expressed through the Bessel functions

$$X_n = C_n x^{1/2} J_{1/(4-\psi)}[\mu(x) \lambda_n] \quad (39)$$

with  $\mu(x) = 2/(4-\psi) \times (4/3\nu_0)^{1/2} x^{(4-\psi)/2}$ . Among the two Bessel functions  $J_{1/(4-\psi)}$  and  $J_{-1/(4-\psi)}$ , only the former one allows  $X_n(x)$  to satisfy the inner boundary condition  $X_n \rightarrow 0$  for  $x \rightarrow 0$ .

We now investigate the behavior of the solution  $X_n$  in the limits of large and small arguments  $\mu(x) \lambda_n$ . Using the asymptotic form of the Bessel function for large arguments (Abramowitz & Stegun 1968)

$$X_n(x) = C_n x^{1/2} \left[ \frac{2}{\pi \mu(x) \lambda_n} \right]^{1/2} \cos[\lambda_n \mu(x) - \pi(6-\psi)/4(4-\psi)]. \quad (40)$$

Comparing this formula with equation (36) we see that  $C_n = [\pi \lambda_n / (4-\psi)]^{1/2}$ . For small values of the argument, the eigenfunction  $X_n$  can be presented as series expansion around 0,

$$X_n(x) = \left[ \frac{\pi \lambda_n}{(4-\psi)} \right]^{1/2} x^{1/2} [\mu(x) \lambda_n / 2]^{1/(4-\psi)} \sum_{k=0}^{\infty} \frac{[-(\lambda_n \mu(x))^2 / 4]^k}{k! \Gamma[(5-\psi)/(4-\psi) + k]}. \quad (41)$$

In fact, it follows from this equation that

$$X_n(x) \propto x \quad (42)$$

when  $\lambda_n \mu(x) \ll 1$ .

The eigenvalues  $\lambda_n$  are determined by the equation

$$\frac{dX_n}{dx} = 0 \quad \text{for} \quad x = x_0. \quad (43)$$

For small  $n = 1, 2$  the eigenvalues are best determined using the series (41), whereas for large  $n$  the asymptotic form (40) is appropriate. Fortunately, even  $\lambda_1$  calculated using the two different methods produces results which differ from each other by less than one percent. For example, the first three terms in series (41) provide an accuracy of  $\lambda_1$  better than 0.1%. The use of these three terms leads us to a quadratic equation for  $u = (4-\psi)z^2/4$  where  $z = \lambda_n \mu(x_0)$ :

$$u^2 - 2(5-\psi)u + 2(5-\psi) = 0. \quad (44)$$

The first root of this equation

$$u_1 = 5 - \psi - [(5 - \psi)^2 - 2(5 - \psi)]^{1/2} \quad (45)$$

allows us to calculate the first eigenvalue. For example, for  $\psi = 1$ ,  $z_1 = 1.25$ , whereas using the second method gives  $z_1 = 1.18$  (see below).

For calculation of the eigenvalues using the eigenfunction form (40) we have the transcendental equation:

$$\tan[z - \pi(6 - \psi)/4(4 - \psi)] = -(2 - \psi)/2z(4 - \psi). \quad (46)$$

The solution of this equation can be written in an analytical form:

$$z \simeq [(n - 1)\pi + \pi(6 - \psi)/4(4 - \psi) - \varepsilon_n], \quad (47)$$

where

$$\varepsilon_n = \frac{2 - \psi}{2(4 - \psi)[(n - 1)\pi + \pi(6 - \psi)/4(4 - \psi)]}. \quad (48)$$

We apply equations (47-48) for calculations of the eigenvalues for any  $n$  because even for the first eigenvalue we have almost the same results using these two methods (compare with Eq. 45).

The Green's function  $K(t)$  can be written using (41) as follows:

$$K(t) \propto \frac{\partial V}{\partial x}(0, t) = D' \sum_{n=1}^{\infty} e^{-\lambda_n^2 t} \lambda_n^{\gamma} X_n(x_0), \quad (49)$$

where  $\gamma = (6 - \psi)/2(4 - \psi)$  and

$$D' = \frac{4}{3} \frac{x_0^2}{\pi^{1/2}} \frac{2}{\mu(x_0)} \left( \frac{4}{3\nu_0} \right)^{1/2(4-\psi)} (4 - \psi)^{-(6-\psi)/2(4-\psi)} \Gamma^{-1}[(5 - \psi)/(4 - \psi)]. \quad (50)$$

Using the asymptotic form of  $X_n$  at  $x = x_0$  (see eq. 40) we can rewrite equation (49) as follows:

$$K(t) \propto \frac{\partial V}{\partial x}(0, t) \simeq D \times \sum_{n=1}^{\infty} \lambda_n^{\gamma} \exp(-\lambda_n^2 t) \cos(b\lambda_n - \pi\gamma/2), \quad (51)$$

where  $b = t_0^{1/2}$  and  $D = D'(3\nu_0/4)^{1/4} x_0^{(\psi-2)/4}$ . As in the case with  $\psi = 2$ , the viscous time is  $t_0$  which in the general case is

$$t_0 = \mu^2(x_0) = \frac{4}{3\nu(R_0)} \frac{4}{(4 - \psi)^2} R_0^2. \quad (52)$$

Thus for  $t \gg \lambda_1^{-2} = (z_1^2/t_0)^{-1}$  or  $t \gg t_0/z_1^2$

$$\frac{\partial V}{\partial x}(0, t) = D \times (z_1^2/t_0)^{\gamma/2} \cos[2(1-\gamma)/\pi(\gamma-3)] \exp(-z_1^2 t/t_0). \quad (53)$$

For  $t \ll t_0/z_1^2$  one should take into account all terms in the series (eq. [51]). As we have already demonstrated in §3, the summation of such a series can be reduced to an integration over  $\lambda$ :

$$\frac{\partial V}{\partial x}(0, t) \simeq D \times \frac{t_0^{1/2}}{\pi} \int_0^\infty \lambda^\gamma \exp(-\lambda^2 t) \cos(b\lambda - \pi\gamma/2) d\lambda, \quad (54)$$

where  $d\lambda \simeq \pi/t_0^{1/2}$ .

Now we proceed with calculation of the integral from equation (54),

$$I = \int_0^\infty \lambda^\gamma \exp(-\lambda^2 t) \cos(b\lambda - \pi\gamma/2) d\lambda = \cos(\pi\gamma/2) I_c + \sin(\pi\gamma/2) I_s, \quad (55)$$

where

$$I_c = \int_0^\infty \lambda^\gamma \exp(-\lambda^2 t) \cos(b\lambda) d\lambda \quad (56)$$

and

$$I_s = \int_0^\infty \lambda^\gamma \exp(-\lambda^2 t) \sin(b\lambda) d\lambda. \quad (57)$$

Expansion of cosine and sine in series and integration over  $\lambda$  leads us to (see also Prudnikov, Bruchkov & Marichev 1981)

$$I_c = \frac{1}{2} t^{-(\gamma+1)/2} \Gamma[(\gamma+1)/2] M[(\gamma+1)/2, 1/2, -b^2/4t] \quad (58)$$

and

$$I_s = \frac{b}{2} t^{-(\gamma+2)/2} \Gamma[(\gamma+2)/2] M[(\gamma+2)/2, 3/2, -b^2/4t]. \quad (59)$$

The asymptotic form of the degenerate hypergeometric function  $M(a, b, z) = e^z z^{a-b} \Gamma(b)/\Gamma(a)$  for large arguments  $z$  (Abramowitz & Stegun 1968) gives us the asymptotic form for integrals  $I_c$  and  $I_s$ :

$$\{I_c, I_s\} \rightarrow (\pi^{1/2}/2) (t_0/4)^{-(\gamma+1)/2} (t_0/4t)^{\gamma+1/2} \exp(-t_0/4t) \quad \text{for } t \ll t_0/4. \quad (60)$$

Finally we have

$$\frac{\partial V}{\partial x}(0, t) \simeq D t_0^{-\gamma/2} \times \pi^{-1/2} (t_0/2t)^{\gamma+1/2} \exp(-t_0/4t) \sin(\pi\gamma/2 + \pi/4) \quad \text{when } t \ll t_0/4. \quad (61)$$

We construct the analytical form of the Green's function  $K(t)$  using the asymptotic forms eq. (53) for  $t \gg t_0$  and eq. (61) for  $t \ll t_0$ , similar to what was done for  $\psi = 2$  in Section 4.1:

$$K(t) = C^{-1} \{ 2.5\pi^{-1/2} (t_0/2t)^{\gamma+1/2} \sin(\pi\gamma/2 + \pi/4) + (z_1^2)^{\gamma/2} \cos[2(1-\gamma)/\pi(\gamma-3)] \} \exp(-t_0/4t - z_1^2 t/t_0), \quad (62)$$

where  $C$  is a normalization constant to make the integral of  $K(t)$  equal to unity. The factor 2.5 in the first term was empirically determined to make this combination of asymptotic forms a better match to the series formulation. This form is primarily a computational convenience. Note that this form breaks down for  $\psi \geq 3$  so we restrict  $\psi$  to be less than 3. A graphical comparison of the series and analytical forms for several values of  $\psi$  can be found in Figure 2.

An important consequence of the previous derivation is that the FRED outburst shape is a natural consequence of the diffusion model. The exponential decay is due to diffusion in a bounded medium, while the fast rise is due to the fact that the probe (X-ray emission from the inner edge of the disk) is located at a distance from the source (accreting material added to the outer edge of the disk). Thus we have derived the outburst shape for a large class of viscosity structures when the viscosity is a function of only the radius.

## 5. Solving The Inverse Problem

In this section, we demonstrate a deconvolution procedure to derive  $A(t)$ , the mass input rate at the outer edge of the disk, and then use  $A(t)$  and  $L_x(t)$  to derive the mass of the disk as a function of time. Now we proceed with general case of the input mass supply in the disk  $Q(R, t)$  which is proportional to  $A(t)$  (see eq. 6). Furthermore, we assume that the mass accretion rate at the inner disk edge is converted with efficiency  $\varepsilon_{\text{eff}}$  into the X-ray luminosity, i.e.  $L_x(t) = \varepsilon_{\text{eff}} \dot{M}(t, R_{in})$ . Thus using the light curve of  $L_x(t)$  we can restore information regarding the input function  $A(t)$  by the deconvolution of the following equation (see eq. 20):

$$L_x(t) = \varepsilon_{\text{eff}} \dot{M}(0, t) = 3\pi \varepsilon_{\text{eff}} \int_0^t A(\tau) K(t - \tau) d\tau. \quad (63)$$

To do this we also assume that the variability time scale for  $A(t)$  is much longer than the viscous time scale  $t_0$ . In other words the support  $T$  of the function  $A(t)$  is much larger than that for  $K(t)$ . Then using the steepest descent method we get from equation (63) that

$$L_x(t) = \varepsilon_{\text{eff}} \dot{M}(0, t) \simeq 3\pi \varepsilon_{\text{eff}} A(\tau_{\text{max}}) \int_0^t K(t - \tau) d\tau \quad \text{for } t \leq T, \quad (64)$$

or

$$L_x(t) = \varepsilon \dot{M}(0, t) \simeq 3\pi \varepsilon_{\text{eff}} A(\tau_{\text{max}}) \int_T^t K(t - \tau) d\tau \quad \text{for } t \geq T, \quad (65)$$

where  $\tau_{\text{max}}$  is the time point for the maximum of  $K(t - \tau)$  in the integration interval. The Green's function  $K(t)$  has a sharp maximum at  $t_*$  (which depends on  $\psi$  and  $t_0$ ) and thus  $\tau_{\text{max}} = 0$  for  $0 \leq t \leq t_*$ ,  $\tau_{\text{max}} = t - t_*$  for  $t_* < t < T$ , and  $\tau_{\text{max}} = T$  for  $T < t < T + t_*$ . With the steepest descent approximation of the convolution (64-65) one can resolve that equation with respect to the input function  $A(t)$ :

$$A(t - t_{\text{off}}) \propto L_x(t) / \int_0^t K(t') dt' \quad \text{for } t \leq T, \quad (66)$$

where  $t_{\text{off}} = \min(t, t_*)$ , and

$$A(t - t_{\text{off}}) \propto L_x(t) / \int_{t-T}^t K(t') dt' \quad \text{for } t \geq T, \quad (67)$$

where  $t_{\text{off}} = \max[(t - T), t_*]$ . Notice that  $t_{\text{off}} = t - \tau_{\text{max}}$ .

To calculate the mass of the disk as a function of time, we make the assumption that the only terms that matter are mass input at the outer boundary of the disk (proportional to  $A(t)$ ) and the mass leaving the disk into the black hole (proportional to  $L_x$ ). Hence the instantaneous change of the disk mass  $M_d(t)$  is determined by the difference between the input function  $A(t)$  and the output function. If we assume that the output mass accretion rate  $\dot{M}(0, t)$  is proportional to the observed luminosity  $L_x(t)$  in accordance with equation (20) and the input function  $A(t)$  is found as a result of deconvolution with the operator  $\mathbf{K}^{-1}$  defined by eqs. (66-67), we can calculate the disk mass as a function of time as follows:

$$M_d(t) \propto \int_0^t \{\mathbf{K}^{-1}[L_x(t)] - L_x(t')\} dt'. \quad (68)$$

It is seen from eqs. (66-67) that  $\mathbf{K}^{-1}$  is a composite operator which shifts and differentially expands the input function  $L_x(t)$ .

## 6. Application to XTE J1118+480

We now apply this formalism to the 2000 January–August outburst of XTE J1118+480. Figure 1 shows a merged 2–12 keV light curve from the ASM on RXTE and the USA Experiment on ARGOS, which together cover the full double-peaked outburst. Only the ASM viewed the initial (FRED) outburst because the notification trigger did not come until the second outburst. During the second outburst intensive observation of the source

commenced. The greater sensitivity of USA is better able to cover the final decline of the source than RXTE.

In order to proceed with the fitting, we need to select a value for the  $\psi$  parameter that defines the radial dependence of the viscosity in the disk. We have no strong physical reason to prefer one value of  $\psi$  over another, so we have chosen  $\psi = 2.8$  primarily because it seems to work relatively well. We found that  $\psi$  close to 3 worked better than  $\psi$  of 1 or 2, so we chose a  $\psi$  slightly less than 3 so that equation (62) would still be valid. In the future, as this method is applied to other sources it may become clear that there is a preferred value for  $\psi$  which is valid for a class of sources.

Figure 3 shows the fit of the Green’s function (eq. [62], with  $\psi = 2.8$ ) to the first outburst. The fit has only two parameters: the viscous timescale  $t_0$ , and the initial time,  $t_{\text{start}}$ . A normalization amplitude is also fitted in Figure 3, but subsequently discarded when the function is normalized to unity. Hence the sole nontrivial parameter (beyond our choice of  $\psi$ ) in the fit is  $t_0$ . The integral of this measured function is found to approximate the shape of the initial rise of the second outburst. The integral has the shape expected from a step function turn on; evidently the second outburst begins with something close to a step function (see Figure 4). This result is a consistency check of the convolution model for the second outburst. In fact, for any input function  $A(t)$  whose support is much larger than that of the Green’s function  $K(t)$ , the shape of the convolution (eq. [63]) begins with the integral of  $K(t)$  multiplied by the initial value of  $A(t)$ . This property of the convolution is a useful tool to distinguish the convolution model of the outburst from other possible models.

Equations (66-67) are used to extract the form of the input function  $A(t)$ . Figure 5 verifies that this is the solution by re-folding the solution with the Green’s function to derive the X-ray luminosity. The solution is smoothed because the convolution with the Green’s function acts as a low-pass filter. Figure 6 displays the inferred mass  $M_d(t)$  and its reciprocal  $M_d^{-1}(t)$  on a plot of the QPO evolution. The interesting result is that the total disk mass is a nearly monotonically decreasing function during the interval when the millihertz QPO frequency is increasing. Despite the fact that the computed evolution of the disk mass looks very similar to the evolution of the X-ray luminosity, the two curves are not identical. The disk mass evolution is obtained from the light curve by the transformation which is effectively a shift transformation.

## 7. Discussion and Interpretation of Observable Quantities

### 7.1. Evolution of the disk mass and $\sim 0.1$ Hz QPO frequency

While Figure 6 is not yet a complete model of the QPO evolution, we argue that it represents a very substantial advance over what was previously available. To date there has been no model which successfully explains the evolution of this low-frequency QPO. If the QPO is some large scale phenomenon in the disk then it should correlate with large scale disk properties. It fails completely to correlate with X-ray luminosity in the sense that  $L_x$  rises and falls while QPO rises monotonically. The function  $M_d^{-1}(t)$ , while not perfect, moves the turnover earlier than that seen for  $L_x$  and hence closer to that observed in the QPO frequency history. We believe that this result, combined with a physical model for the QPO evolution represents a significant improvement in our understanding of the observed QPO. Note that our model included several simplifying assumptions which when corrected may account for the remaining differences.

We may now reconsider the global oscillation model (TO00,) in which a monotonic dependence of  $M_d^{-1}$  on the QPO frequency  $\nu_0$  is derived, giving  $M^{-1} \propto \nu_0^2$  (see eqs. [4, 7] there). The observed dependence is flatter than the predicted one; that discrepancy could be a result of our assumption of constant conversion efficiency  $\varepsilon_{\text{eff}}$  of the mass accretion rate (in fact, the surface density) at the inner disk edge into X-ray luminosity. It is possible that the inner radius of the disk changes along with the outer disk radius, causing the variation of  $\varepsilon_{\text{eff}}$ .

The global oscillation is a vertical displacement of a large portion of the disk. The exact mechanism whereby this modulates X-ray (as well as optical and EUV) emission to produce a QPO remains unclear. One possibility is that the modulation is geometrical in nature, *e.g* from varying obscuration of the hot inner portions of the disk. This would require the system to be at a fairly high inclination, as found by Wagner et al. (2001) for this source. In addition, for this idea to be viable the corona would have to be somewhat limited in extent. Thus if the relevant disk oscillations were at  $10^3 R_S$  (where  $R_S$  is the Schwarzschild radius) and the corona were confined to less than  $10^{2-3} R_S$  the geometrical model could work. Other scenarios could include having the disk brightness respond in some way to the global oscillation.

## 7.2. Disk kinematic viscosity estimate and turbulent disk scale

The best-fit parameter  $t_0 = 48$  d in the Green's function from equation (62) (see Fig. 3) allows us to derive the kinematic viscosity value because  $t_0 = 16R_0^2/3\nu(R_0)$  from equation (49). Thus the kinematic viscosity is  $\nu \sim 2 \times 10^{15}$  cm<sup>2</sup> s<sup>-1</sup> since  $R_0 \sim 4 \times 10^{10}$  cm (from eq. [10] in TO00 for  $R_{\text{out}}$  and using  $m = M/M_{\odot} = 7$  and the orbital period 4.1 hours). This estimate leads to  $l_t = 6 \times 10^9$  cm if we assume that  $v_t$  is of order of a thermal velocity at the outer edge of the disk, i.e.  $v_t \sim 10^6$  cm s<sup>-1</sup>.

## 8. Discussion and Conclusions

Here we have presented a detailed mathematical analysis of the diffusion propagation model for X-ray outbursts. We investigated the intrinsic properties of the disk density evolution equation (5) in a general case. We have analyzed the diffusion models determined by the disk kinematic viscosity dependence on the radius. We have demonstrated that the Green's (response) function is characterized by the fast rising and exponential decay parts (FRED shape) and that it is an intrinsic property for a wide class of diffusion models. Similar results were obtained by Sunyaev & Titarchuk (1980) for photon diffusion models. Particularly, the light curve of the instant turn-on of a photon source placed in the center of a spherical cloud (or the center disk plane) has a typical FRED type shape (Figs. 1-2 there).

The success in fitting the diffusion model to the observed light curve is very promising. We have examined the case where the viscosity is a power law function of position in the disk. We note that a dependence of viscosity on surface density is also possible, but this will make the problem nonlinear (see Lyubarskii & Shakura 1987 and Lyubarskii 1997 for details).

We showed in §5 that the steepest descent method can be employed to solve the inverse problem (a deconvolution) and extract the input mass accretion function  $A(t)$  using the observed X-ray luminosity evolution. Such a deconvolution is possible because the inner mass accretion rate and the X-ray rate production are related to each other and the timescale for viscous diffusion is short enough compared to the timescale of the outburst. Using the derived  $A(t)$  as the source term and  $L_x$  as a measure of the mass lost from the disk into the black hole, we derived the mass of the disk as a function of time. This appears to inversely correlate with the observed QPO frequency as would be expected from the global disk oscillation model, but the correlation is not perfect.

There are several factors that have been ignored for simplicity in this initial treatment which could modify the derived disk mass as a function of time: (1) a changing efficiency of

the conversion of mass to  $L_x$  at the inner edge of the disk, (2) an effective viscous time ( $t_0$ ) which varies with time, and (3) an additional sink for disk matter such as a jet. We realize that the model is imperfect but we think that the initial application is encouraging and that further study and application to other sources is warranted.

We conclude by summarizing the main results of the diffusion model. (1) The asymptotic form (eq. [62]) is characterized by the exponential rise when the escape time is less than the diffusion timescale from the location of mass injection. The same asymptotic form would be seen for a semi-infinite medium and thus is determined by the escape boundary condition (in our case at  $R = R_{\text{in}}$ ) and the location of the mass source. This asymptotic form is insensitive to the size of the medium. The second asymptotic form is characterized by an exponential decay with the viscous timescale  $t_0$  which is a signature of the bounded medium (in our case, a disk) rather than any specific model of the diffusion. (2) The “FRED” shape of the first outburst of XTE J1118+480 is in good agreement with the diffusion Green’s function form (eq. [62]), for which only one free parameter  $t_0$  is important. The variation of the viscosity index  $\psi$  leads to a change of  $t_0$  but the “FRED” shape remains.

This particular result is very important because it is closely related to the intrinsic property of the diffusion Green’s function. (3) The value of the parameter  $t_0$  has a physically plausible value for the viscous timescale of the disk and ultimately can be applied to the calculation of the disk turbulent scale using certain assumptions regarding the disk size and the turbulent velocity (4). The rise of the second outburst follows the form expected for a step function input, the integral of the Green’s function. It is worthwhile to emphasize that the shape of this rise is precisely the integral of the Green’s function derived from the first outburst. (5) The derived mass varies approximately inversely with the QPO frequency. (6) Similar X-ray luminosity and QPO evolution would be expected in other sources with similar behavior, and in fact is seen in X1354–644 and GRO J1719–24 (Brocksopp et al. 2000). In our model, the rising QPO frequency is a signature of the accretion disk mass decreasing as it disappears into the black hole. If QPO frequency varies inversely with disk mass throughout the outburst there is a possibility that early detection – before the mass reaches its maximum – might find the QPO when its frequency is still decreasing. Both the relatively low brightness in the earliest stages of outbursts and the difficulties of prompt response would appear to have selected against detection of this effect to date.

We would like to acknowledge the many helpful comments of an anonymous referee. Basic research in X-ray Astronomy at the Naval Research Laboratory is supported by the Office of Naval Research. This work was performed while RMB held a National Research Council Research Associateship Award at NRL. This paper made use of quick-look results provided by the ASM/RXTE team (see <http://xte.mit.edu>).

## REFERENCES

Abramowitz, M., & Stegun, I. A. 1968, Handbook of Mathematical Functions (New York: Dover)

Bath, G. T., & Pringle, J. E. 1981, MNRAS, 194, 967

Brocksopp, C., et al. 2000, MNRAS, in press (astro-ph/001145)

Chakrabarti, S. K., & Titarchuk, L. G. 1995, ApJ, 455, 623

Chen, W., Shrader, C. R., & Livio, M. 1997, ApJ, 491, 312

Cannizzo, J. K., Chen, W., & Livio, M. 1995, ApJ, 454, 880

Dubus, G., Hameury, J-F., & Lasota, J-P. 2001, A&A in press (astro-ph/0102237)

Dubus, G., Kim, R. S. J., Menou, K., Szkody, P., & Bowen, D. V. 2000, ApJ, submitted, astro-ph/0009148

Fender, R. P., Hjellming, R. M, Tilanus, R. J., Pooley, G. G., Deane, J. R., Ogle, R. N., & Spencer, R. E. 2000, MNRAS, submitted

Haswell, C. A., Skillman, D., Patterson, J., Hynes, R. I., Cui, W. 2000 IAU Circ 7427

Hynes, R. I., Mauche C. W., Haswell, C. A., Shrader, C. R., Cui W., & Chaty, S. 2000, ApJ, 539, L37

King, A.R., & Ritter, H. 1995, MNRAS, 293, L42

King, A. R., 1995, in X-ray Binaries, ed. W. H. G. Lewin, J. van Paradijs & E. P. J. van den Heuvel (Cambridge: Cambridge Univ. Press), 419

Kuulkers, E. 2001, Astron. Nachr. submitted (astro-ph/0102066)

Lasota, J-P. 2001, New Astronomy, submitted (astro-ph/0102072)

Lyubarskii, Yu. E. 1997, MNRAS, 292, 679

Lyubarskii, Yu.E., & Shakura, N.I. 1987, Sov. Astron. Lett., 13, 386

McClintock, J., Garcia, M., Zhao, P., Caldwell, N, & Falco, E. 2000, IAUC 7542

McClintock, J., Garcia, M., Caldwell, N, Falco, E. E., Garnavich, P. M., & Zhao, P. 2001, ApJ, in press (astro-ph/0101421)

Menou, K., Esin, A., Narayan, R., Garcia, M., Lasota, J-P., & McClintock, J. 1999, ApJ, 520, 276

Revnivtsev, M., Sunyaev, R. A. & Borozdin, K.I. 2000, A&A, 361, L37

Shahbaz, T., & Kuulkers, E. 1998, MNRAS, 295, L1

Shakura, N. I., & Sunyaev, R. A. 1973, A&A, 24, 337

Sunyaev, R. A., Titarchuk, L. G. 1980, A&A, 86, 121

Titarchuk, L., Mastichiadis, A., & Kylafis, N. 1997, ApJ, 487, 834

Titarchuk, L., & Osherovich, V. 1999, ApJ, 518, L95 (T099)

Titarchuk, L., & Osherovich, V. 2000, ApJ, 542, L111 (T000)

Wagner, R. M., Foltz, C. B., Shabaz, T., Casares, J., Charles, P. A., Starrfield, S. G., & Hewett, P. 2001, submitted (astro-ph/0104032)

Warner, B. 1995 in Cataclysmic Variable Stars (Cambridge: Cambridge University Press)

Wood, K., Ray, P. S., Bandyopadhyay, R. M., et al. 2000, ApJ, 544, L45

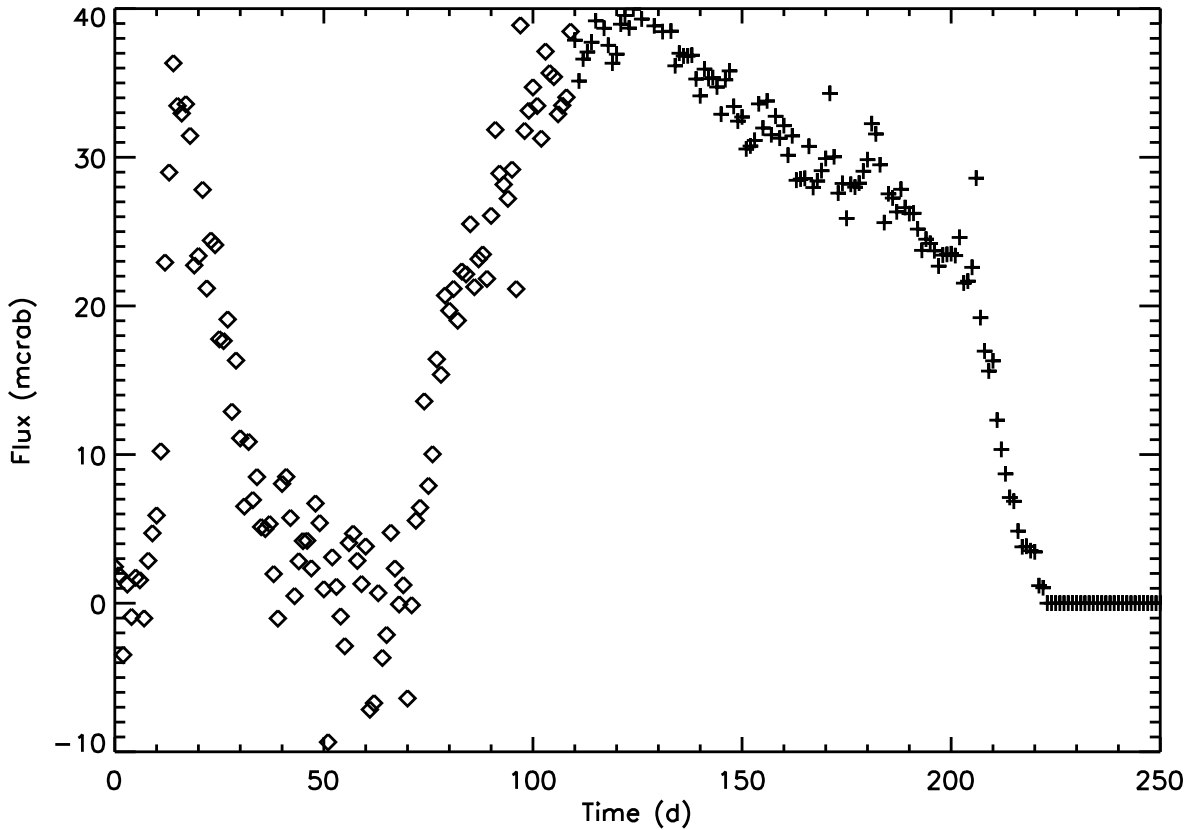


Fig. 1.— Complete outburst light curve of XTE J1118+480. The time axis is labeled as days since 1999 December 23. Diamonds are data from the RXTE/ASM and crosses are from USA. The greater sensitivity of USA is reflected in reduced scatter after day 110 where the USA data begin. The data have been interpolated and re-gridded so as to give one data point per day.

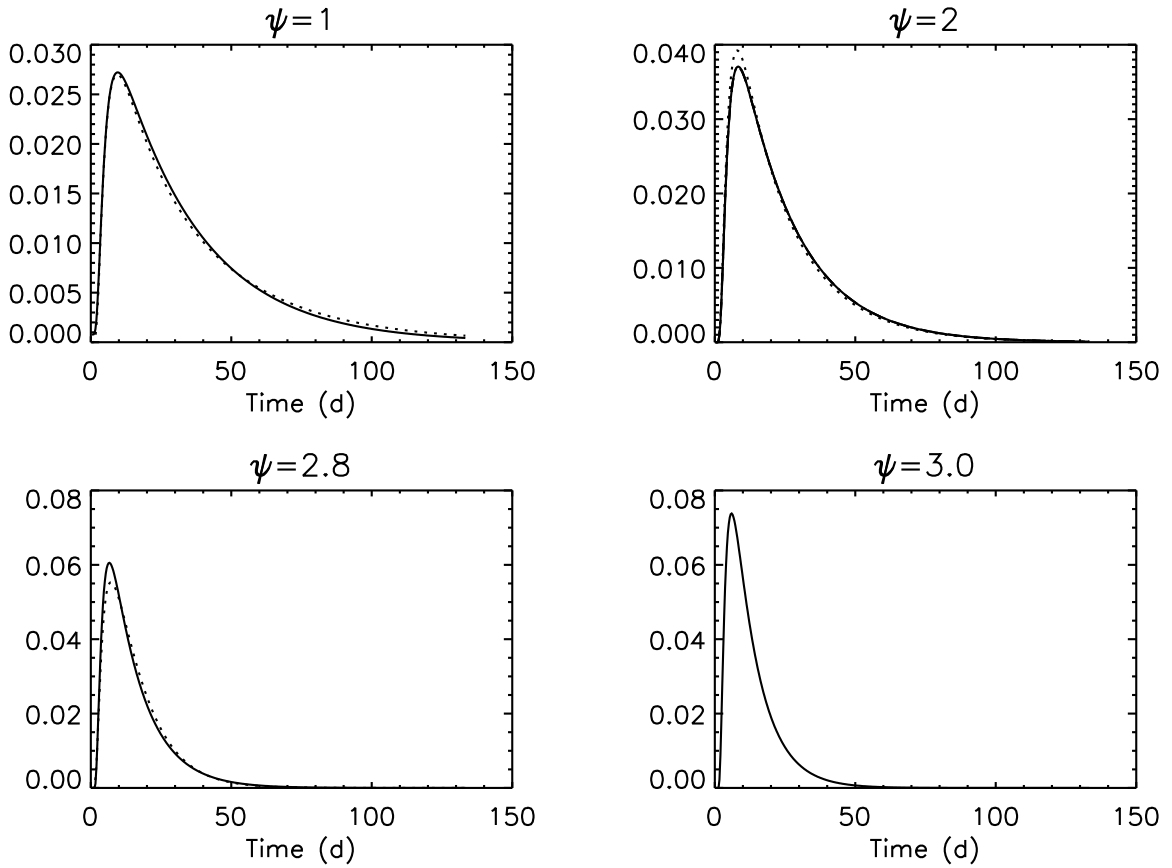


Fig. 2.— Comparison of the Green’s Function  $K(t)$  for various values of  $\psi$ . The solid line is the series formulation (eq. [51]) and the dotted line is the combination of asymptotic forms (eq. [62]). There is no dotted line in the bottom right panel because equation (62) breaks down for  $\psi \geq 3$ .

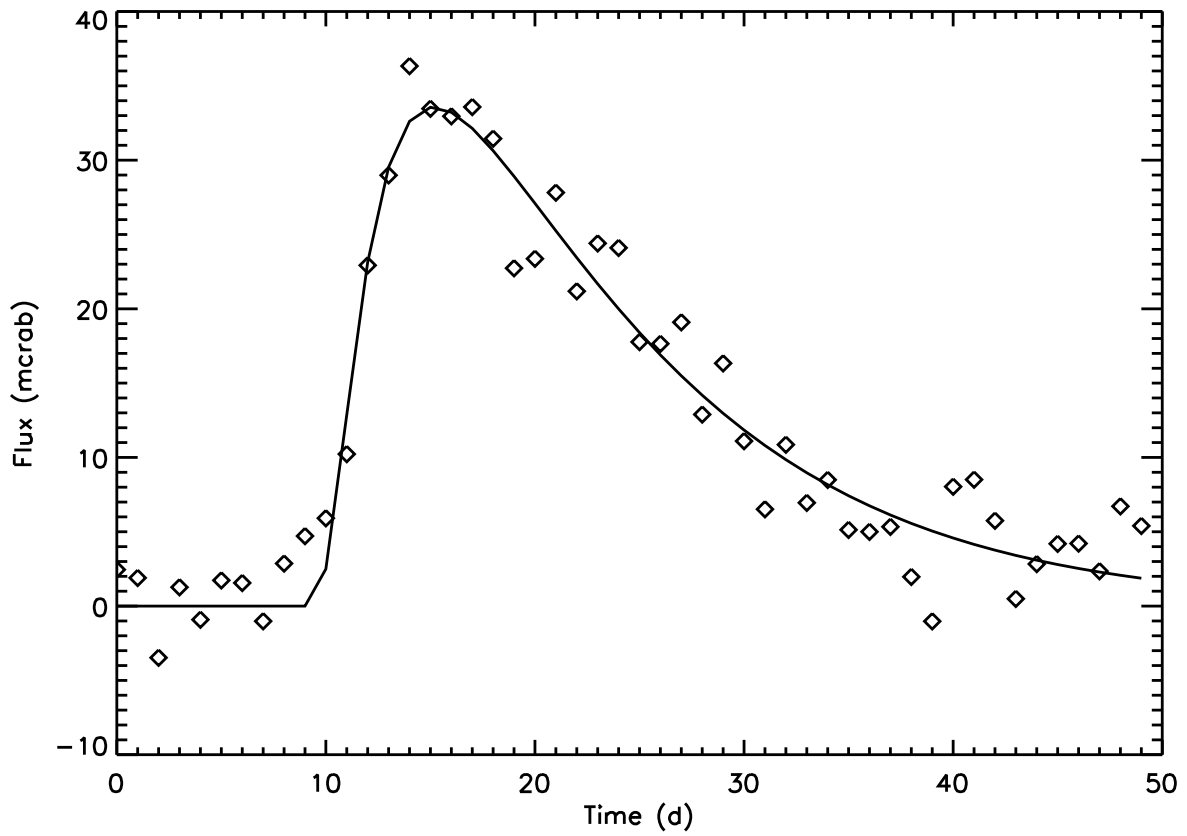


Fig. 3.— Fit of Green’s function (eq. [62]) to initial outburst. For the fit, we have chosen  $\psi = 2.8$ . Other than the trivial amplitude and start time, there is only one free parameter,  $t_0$ .

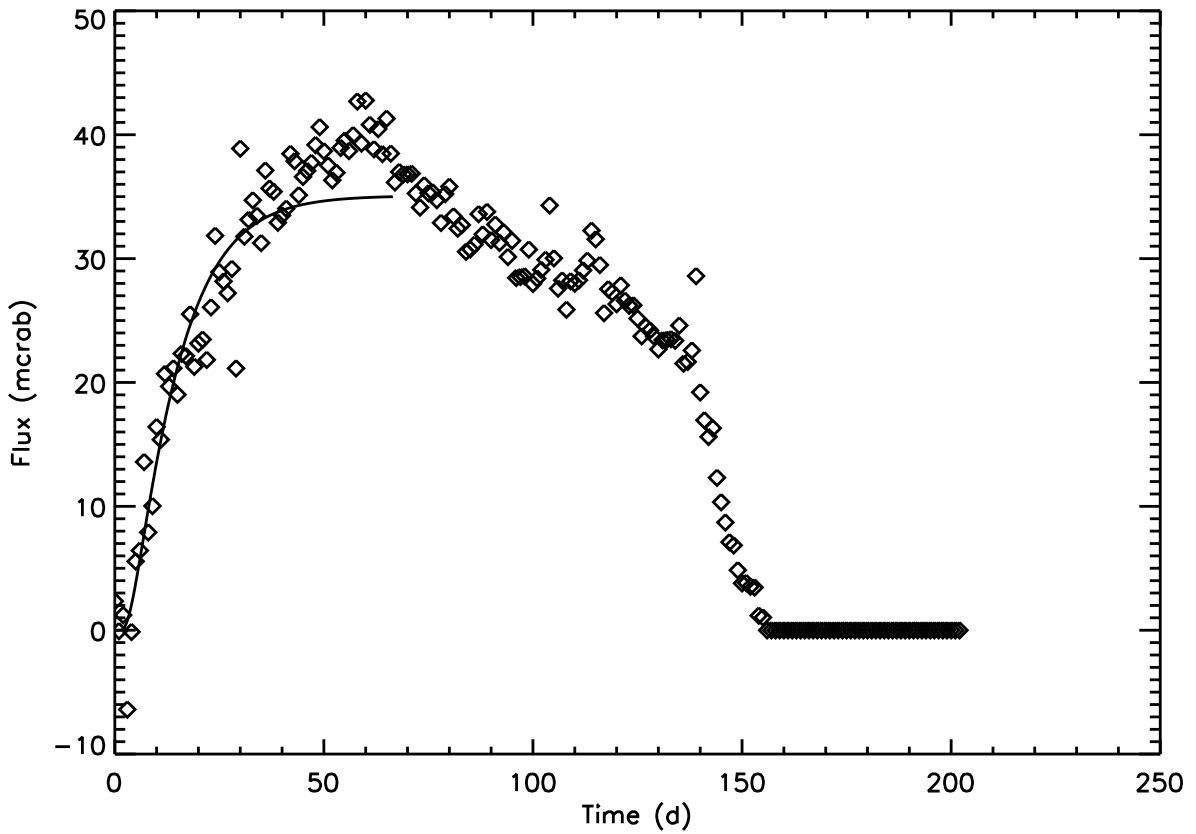


Fig. 4.— Plot of complete second outburst showing integral of the best fit Green's function from the first outburst as a solid line. This is the shape that would be expected for a step function turn on of the mass transfer causing the second outburst.

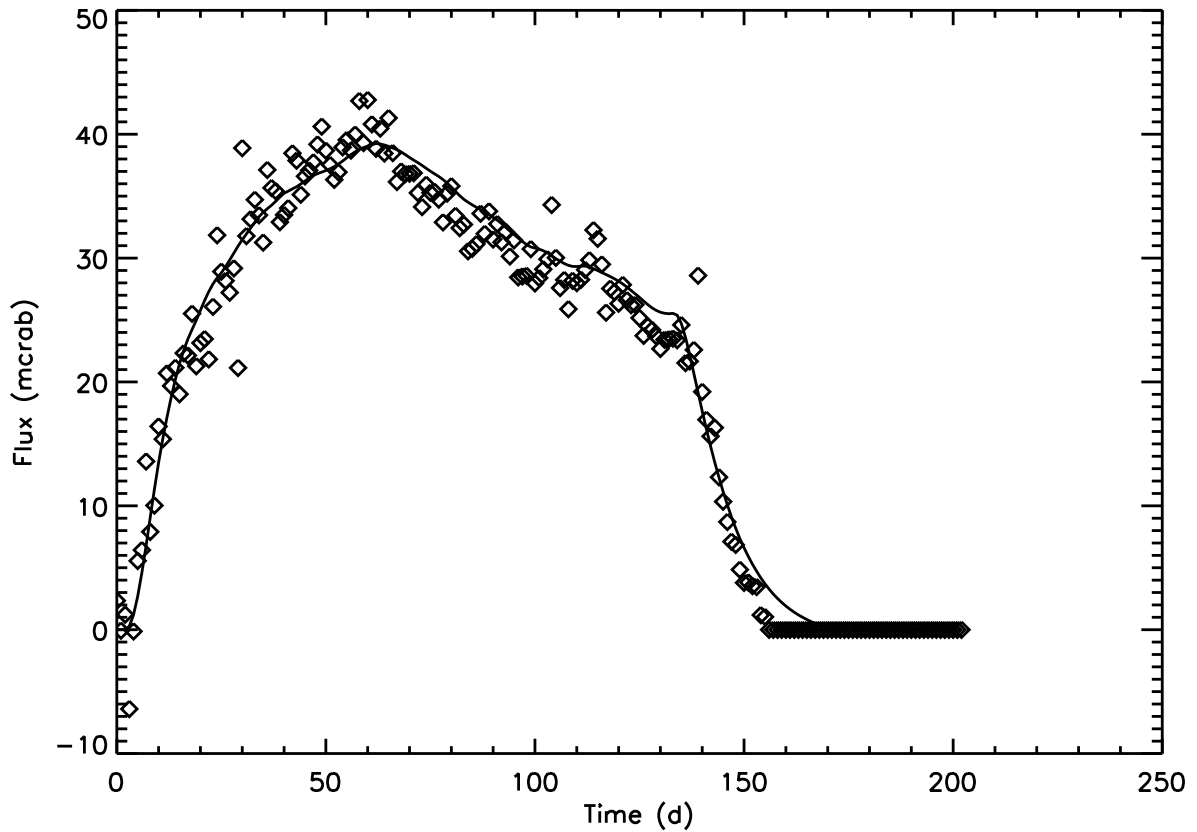


Fig. 5.— Convolution of derived  $A(t)$  with Green's function to get estimated (smoothed)  $L_x(t)$ . The solution process integrates and smooths the input like a low pass filter.

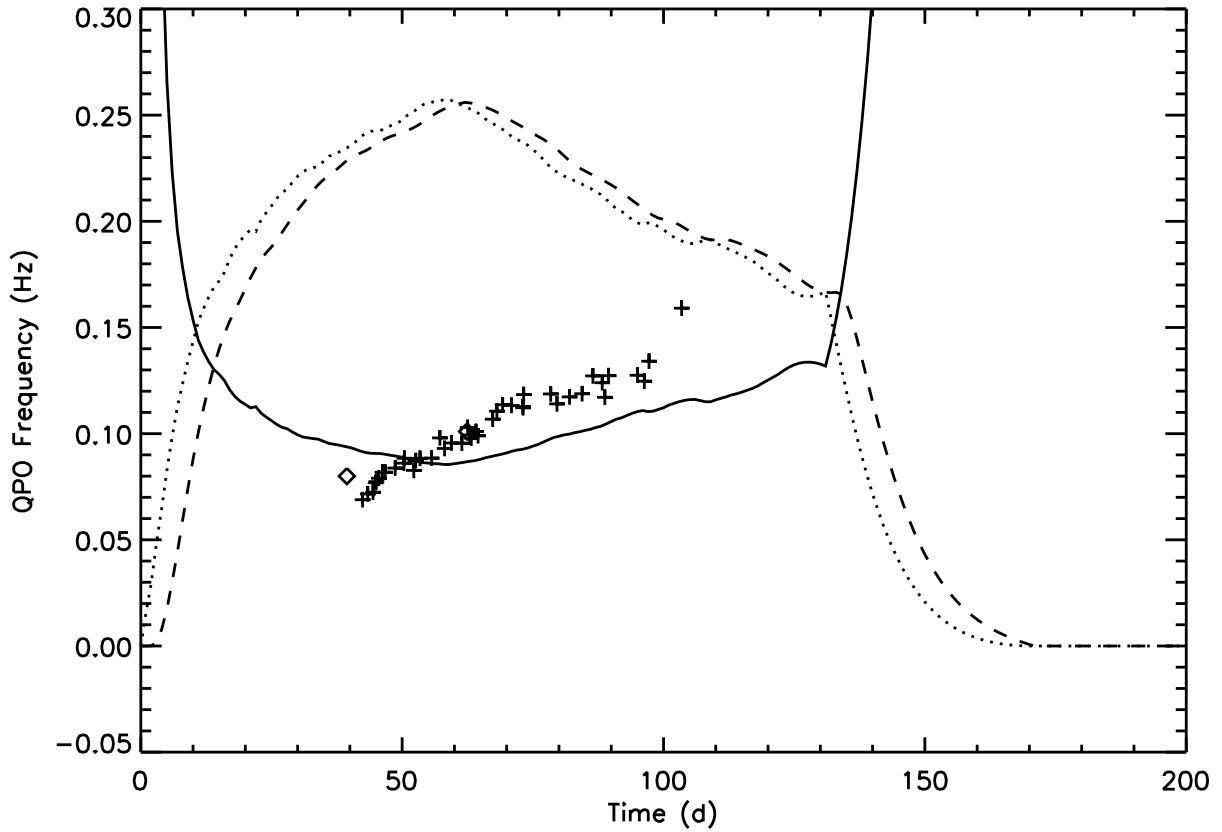


Fig. 6.— Comparison of the QPO frequency evolution with the derived mass of the disk. The points are the QPO frequency according to the left axis (crosses are X-ray determined QPO frequencies from Wood et al. (2000) and diamonds are optically determined QPO frequencies from Haswell et al. (2000) and J. Patterson & D. Skillman, private communication). The dotted line and the solid line are  $M_d$  and  $M_d^{-1}$  respectively with arbitrary scale factors to put them on the same scale as the QPO frequency. The ripple in  $M_d$  and  $M_d^{-1}$  derives from the scatter in the daily X-ray flux measurements, propagated through the inversion process. The dashed line is the smoothed  $L_x$  included to highlight the shift between  $L_x$  and  $M_d$ .